Supplementary Information

Antibody-independent mechanisms regulate the establishment of chronic *Plasmodium* infection

Thibaut Brugat[1]*†, Adam James Reid[2]*†, Jingwen Lin[1], Deirdre Cunningham[1,] Irene Tumwine[1], Garikai Kushinga[1], Sarah McLaughlin[1], Philip Spence[4]‡, Ulrike Böhme[2], Mandy Sanders[2], Solomon Conteh[5], Ellen Bushell[2], Tom Metcalf[2], Oliver Billker[2], Patrick E. Duffy[5], Chris Newbold[2,3], Matthew Berriman[2] & Jean Langhorne[1]*.

[1] The Francis Crick institute, London NW1 1AT, UK.

[2] Wellcome Trust Sanger Institute, Hinxton, Cambridge CB10 1SA, UK.

[3] Weatherall Institute of Molecular Medicine, Oxford OX3 9DS, UK

[4] MRC National Institute for Medical Research, London NW7 1AA, UK.

[5] Laboratory of Malaria Immunology and Vaccinology, National Institute of Allergy and Infectious Diseases, National Institutes of Health, Rockville, MD, United States of America.

†These authors contributed equally to the work

*Corresponding Authors: Jean Langhorne and Thibaut Brugat, Francis Crick institute, London NW1 1AT. jean.langhorne@crick.ac.uk and thibaut.brugat@crick.ac.uk, tel: +44 208 816 2558; Adam James Reid, Wellcome Trust Sanger Institute, Genome Campus, Hinxton, Cambridgeshire, CB10 1SA. ar11@sanger.ac.uk, tel: +44 1223 494810.

‡Present Address: Institute of Immunology and Infection Research (IIIR), School of Biological Sciences, The University of Edinburgh, United Kingdom

Supplementary Figures

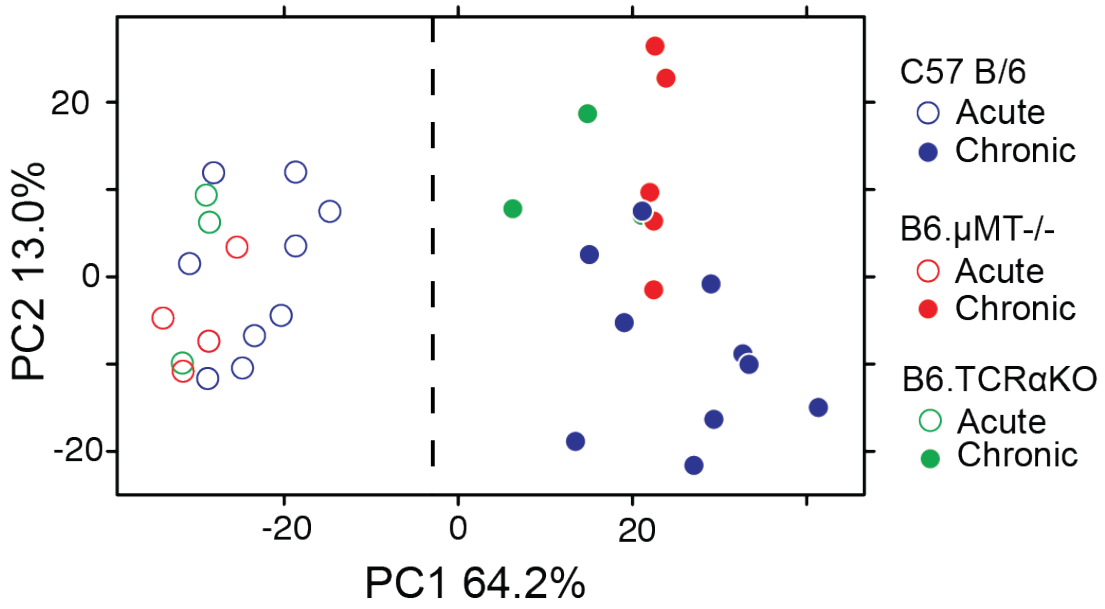

Supplementary Figure 1. Principal Components Analysis plot of transcriptomes from *P. chabaudi* AS parasites collected at acute and chronic phases of infection in wild-type and mutant mice. Wild-type C57Bl/6 (blue), B6.µMT-/- (red) and TCRα-/- (green) mice were infected by mosquito bites. Parasite mRNA were collected during the acute (open circles) and chronic (close circles) of infection. Gene expression does not differ greatly between parasites in wild-type (blue), µMT-/- (red) or TCRaKO (green) mice. Changes between the acute and chronic phases are consistent between the three genetic backgrounds.

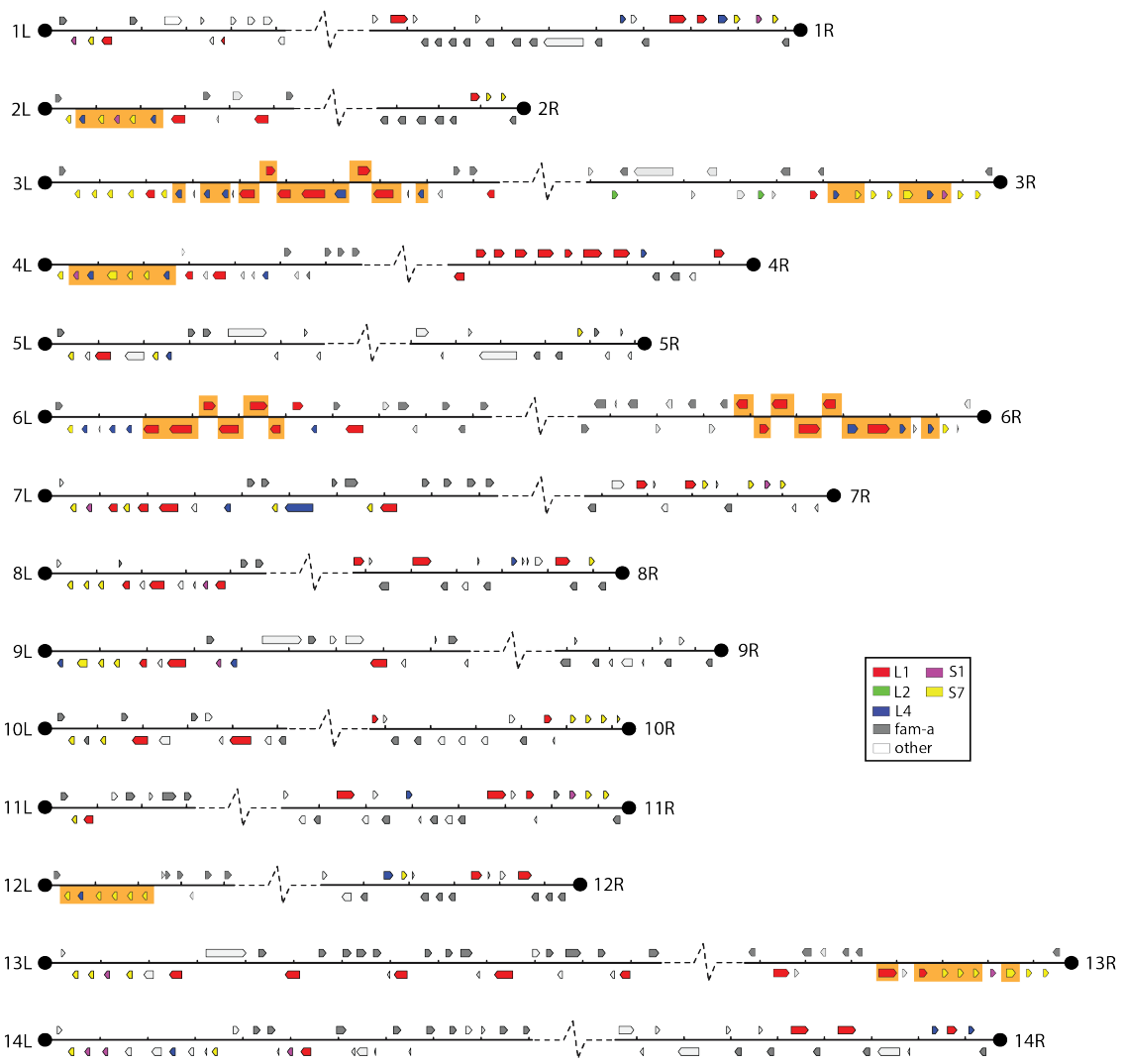

Supplementary Figure 2. Structure of all subtelomeres in the v3 *P. chabaudi* AS genome assembly

Pir genes are shown in the context of the subtelomeric region from the telomeric repeats to the last *pir* or *fam-a* gene. Those genes co-expressed across mice over the course of infection are highlighted in orange. Genes are coloured by subfamily.

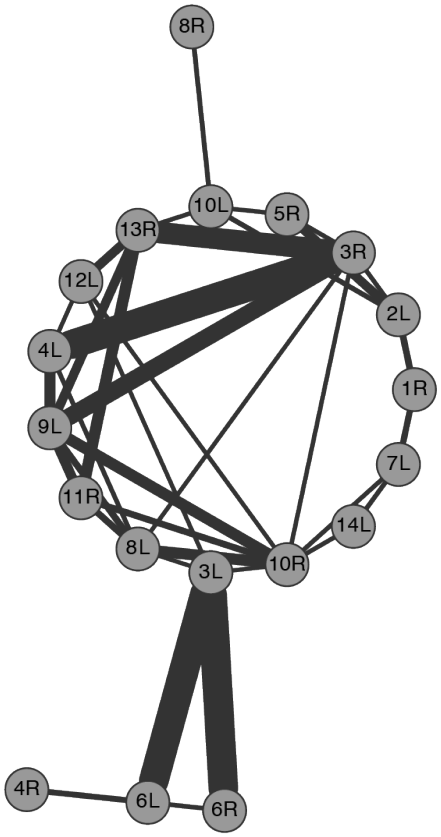

Supplementary Figure 3. Similarity of *pir* genes between different subtelomeres.

Protein sequences for all *pir* genes were BLASTed against each other (blastall 2.2.25; E >= 0.01; sequence identity >= 80%). Matches between a node and itself were ignored. For any two nodes the greatest match length was taken, rather than summing the match lengths for the two nodes. For each pair of subtelomeres, the total length of the hits was determined and used as the edge weight in the graph. Edges with <300 amino acids were excluded. The maximum number of amino acids was 1972. The figure shows two particularly similar arrays of *pir* genes: L1-rich 3L, 6L, 6R and S7-rich 3R, 13R, 4L and 9L. Visual inspection of the subtelomeres suggests that 4R is similarly rich in L1 *pirs* as the first group, while 12L and 2L are rich in S7s like the latter group. 3L has both L1-rich and S7-rich regions, which explains why it links the two principal subtelomere types.

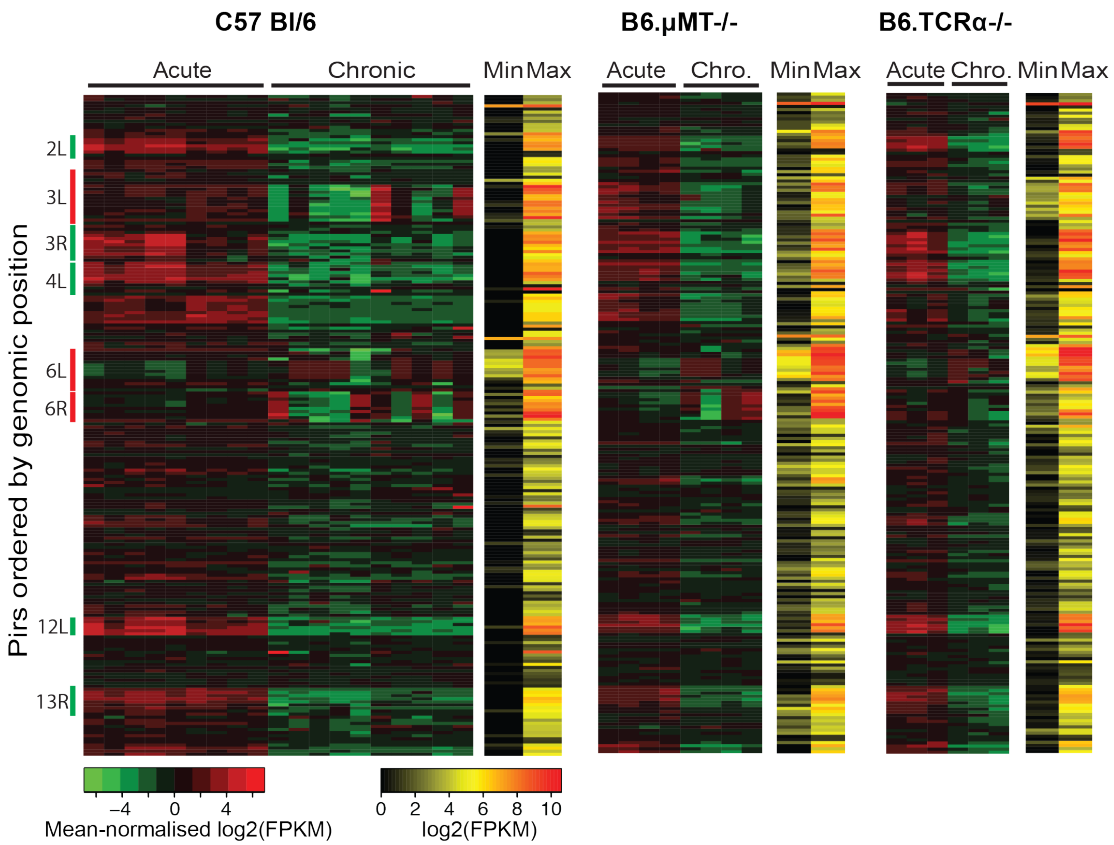

Supplementary Figure 4. Heatmap of *pir* gene expression at ChAPL and AAPL loci.

10 wild-type C57Bl/6 mice, 5 B6.µMT-/- mice and 3 TCRα-/- mice were infected by mosquito bites. Each column represents values obtained from an individual mouse. The first nine columns represent samples collected during the acute phase. The next ten columns represent samples collected during the chronic phase. *Pir* genes were ordered by their position in the genome. On the side, numbers indicate chromosomes and letters indicate the location on that chromosome: L for left hand end, R for right hand end. ChAPLs and AAPLs are highlighted. For each gene, red represents its maximal expression, green its minimal expression. The maximum and minimum values for each gene are shown in a separate heatmap.

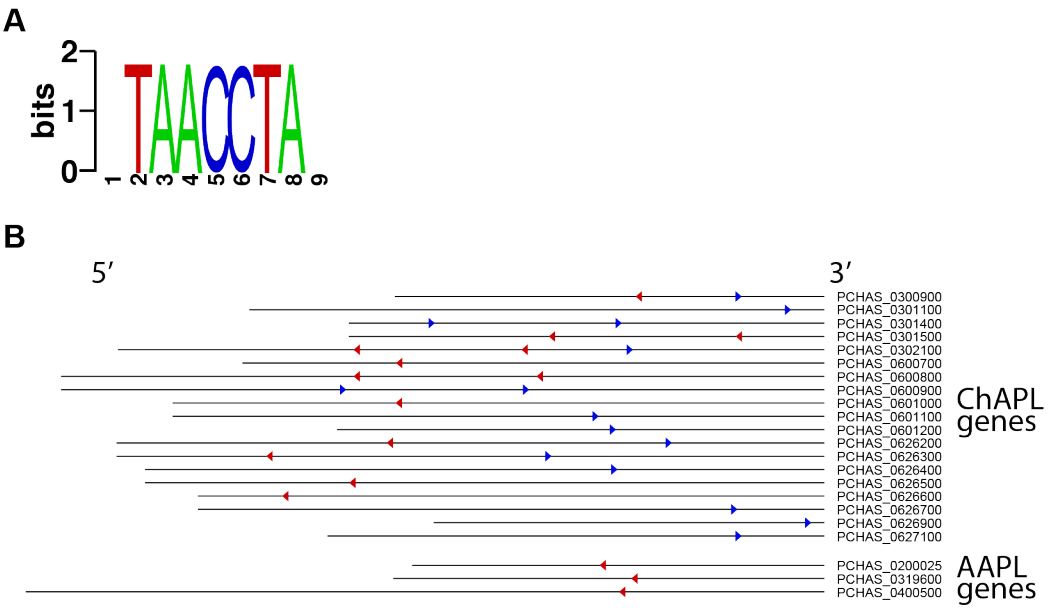

Supplementary Figure 5. A DNA sequence motif associated with the upstream, intergenic regions of ChAPL genes. (A) Sequence logo of the identified motif. Z-score 23.9, robustness 7/10 (B) Motif location in intergenic region (excluding UTRs) upstream of *pir* genes from ChAPLs and AAPLs. Blue arrows indicate an instance of the TAACCTA motif on the forward strand, red arrows the reverse strand. The motif occurs in 19/27 ChAPL genes tested. Reliable upstream intergenic regions could not be determined for all genes: there are a total of 32 ChAPL and 28 AAPL genes. The motif rarely occurs upstream of AAPL genes (3/22 tested) and only in the reverse orientation. Motifs in the forward orientation tend to occur closer to the transcription start site (TSS) of the gene, whereas those in the reverse orientation are more distal to the TSS.

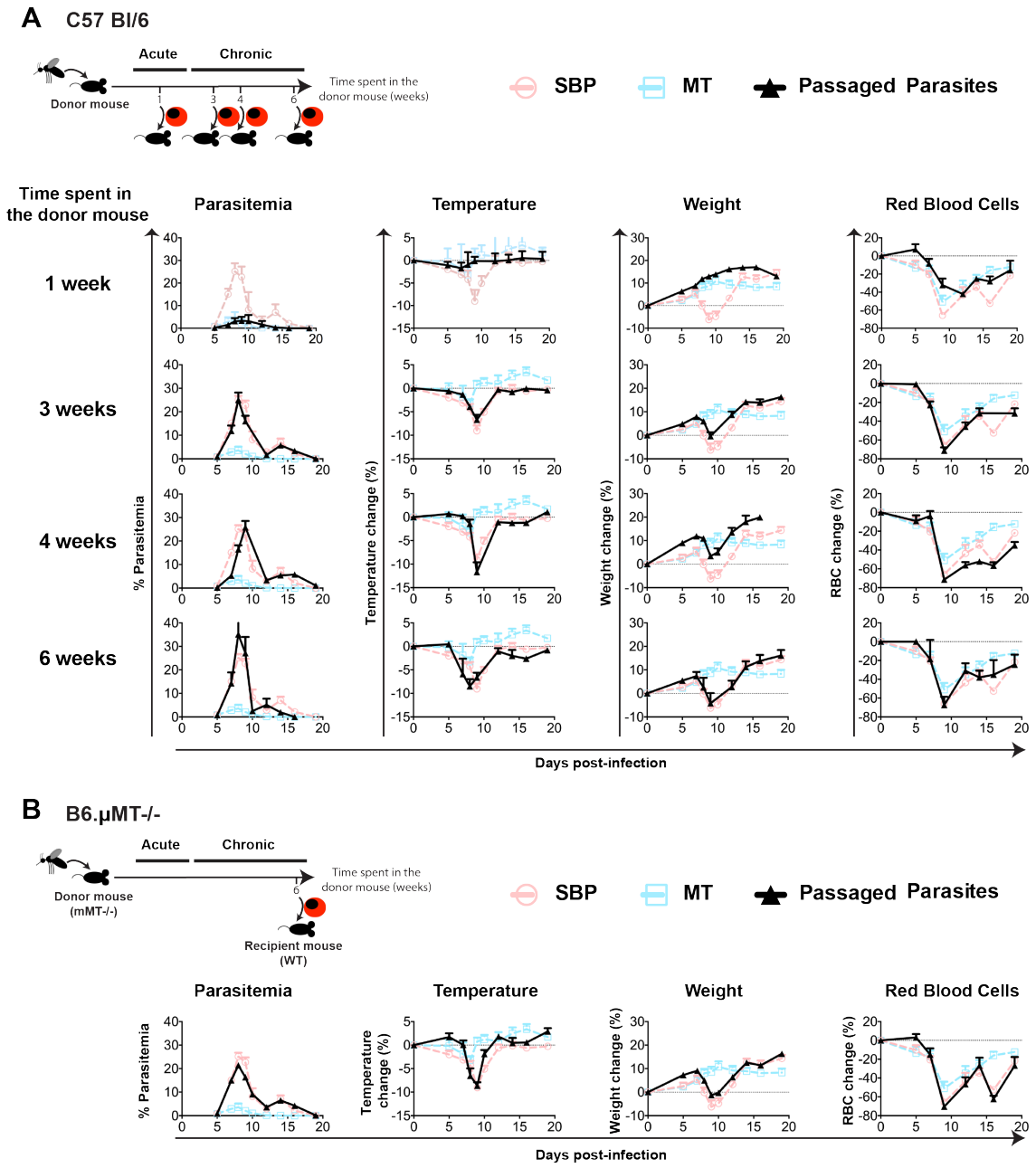

Supplementary Figure 6. Course of infections initiated with acute and chronic parasites

(A) Wild-type C57Bl/6 donor mice were infected by mosquito bites and parasites were subsequently passaged into naïve recipient mice after one, three, four or six weeks (n=15

mice per group). (B) B6.μMT donor mice were infected by mosquito bites and parasites were passaged into naïve wild type recipient mice after six weeks (n= 5 mice). For both experiments, we show parasitaemia and changes in temperature, weight, and red blood cell density over the course of infection in recipient mice compared to wild type mice directly infected by mosquito bites (MT; light blue dotted line) or with serially blood passaged parasites (SBP; light red dotted line). Each dot represents the average ±SEM.

94

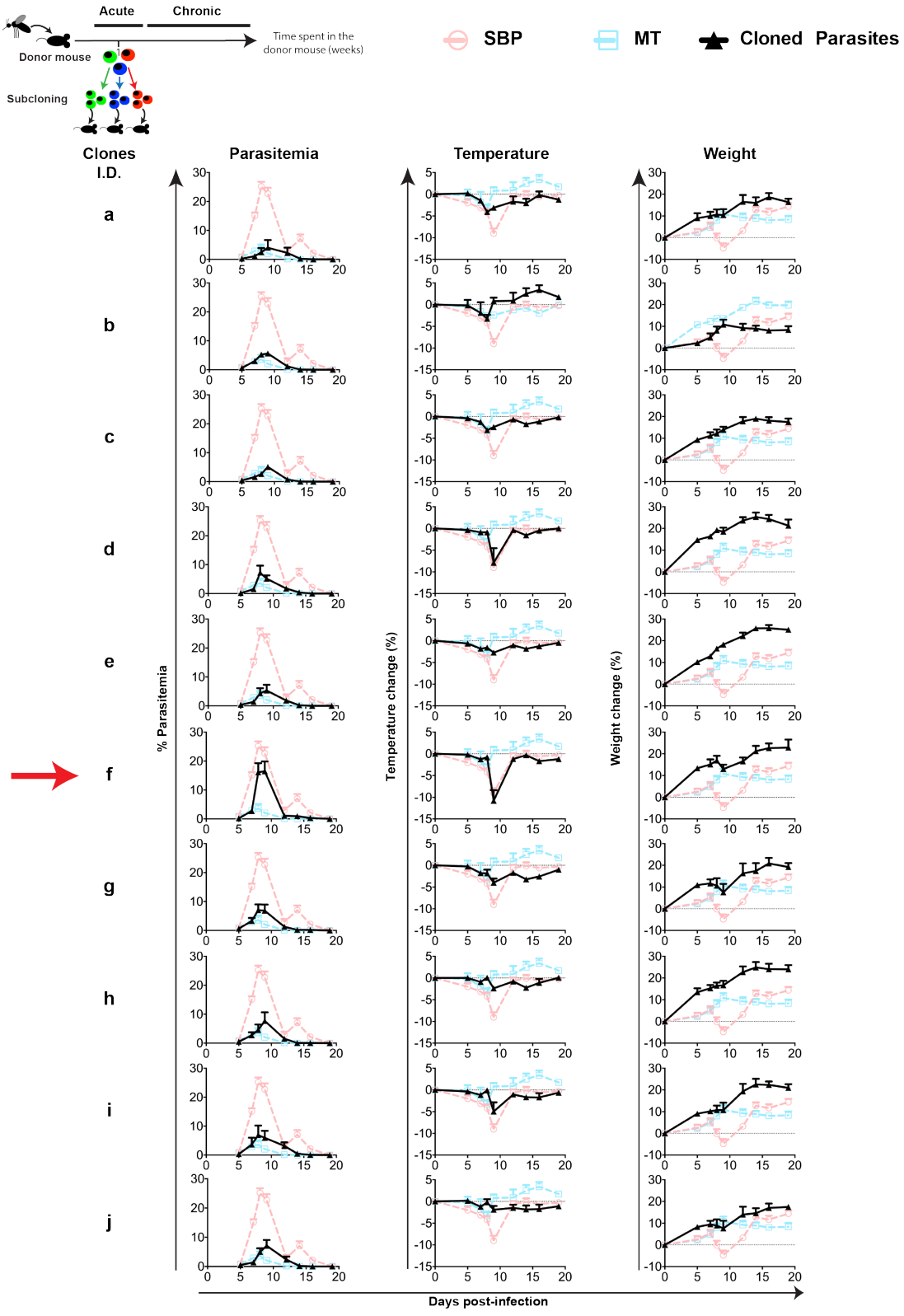
Acute
Chronic
Time spent in the donor mouse (weeks)
Donor mouse
Subcloning
SBP
MT
Cloned Parasites
Clones I.D.
Parasitemia
Temperature
Weight
a
b
c
d
e
f
g
h
i
j
% Parasitemia
Temperature change (%)
Weight change (%)
Days post-infection

95
96

Supplementary Figure 7. Course of infections initiated with acute clones

One donor mouse was infected by mosquito bites. Individual *P. chabaudi* AS parasites were subsequently cloned during the acute phase of infection. After their expansion, recipient mice were infected with clonal populations of parasites (n= 5 mice per group). For each clonal infection, we show parasitaemia and changes in temperature and weight over the course of infection in recipient mice compared to mice directly infected by mosquito bites (MT; light blue dotted line) or with serially blood passaged parasites (SBP; light red dotted line). Each dot represents the average ±SEM. The red arrow indicates the clone derived from the acute phase that reached relatively high parasitaemia and induced significant temperature loss in naïve mice.

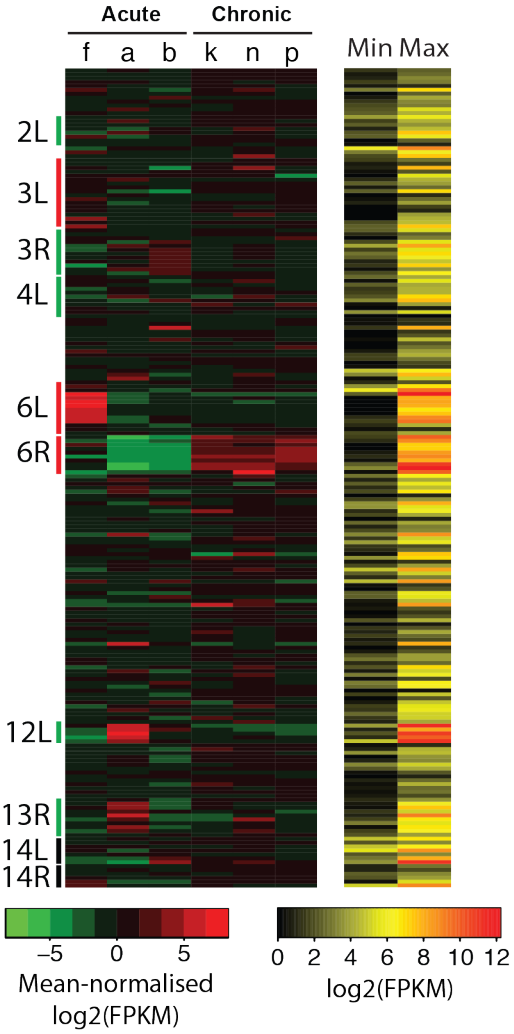

Supplementary Figure 8. Heatmap of *pir* gene expression at ChAPLs and AAPLs in three acute and three chronic clones.

One donor mouse was infected by mosquito bites. Individual *P. chabaudi* AS parasites were subsequently cloned during the acute and chronic phase of infection. After their expansion, recipient mice were infected with clonal populations of parasites (n= 3 mice per group). For each clonal infection, parasite RNA were extracted during the late trophozoite stage after completion of seven cycles of schizogony. Each column represents the values obtained from 3 individual mice infected with the same clonal population of

parasites. The first three columns represent clones from the acute phase, the next three columns represent clones from the chronic phase. *Pir* genes were ordered by their position in the genome. On the side, chromosomes numbers are indicated as well as the location on that chromosome: L for left hand, R for right hand. ChAPLs and AAPLs are highlighted. For each gene, red represents its maximal expression, green its minimal expression. The maximum and minimum values for each gene are shown in a separate heatmap.

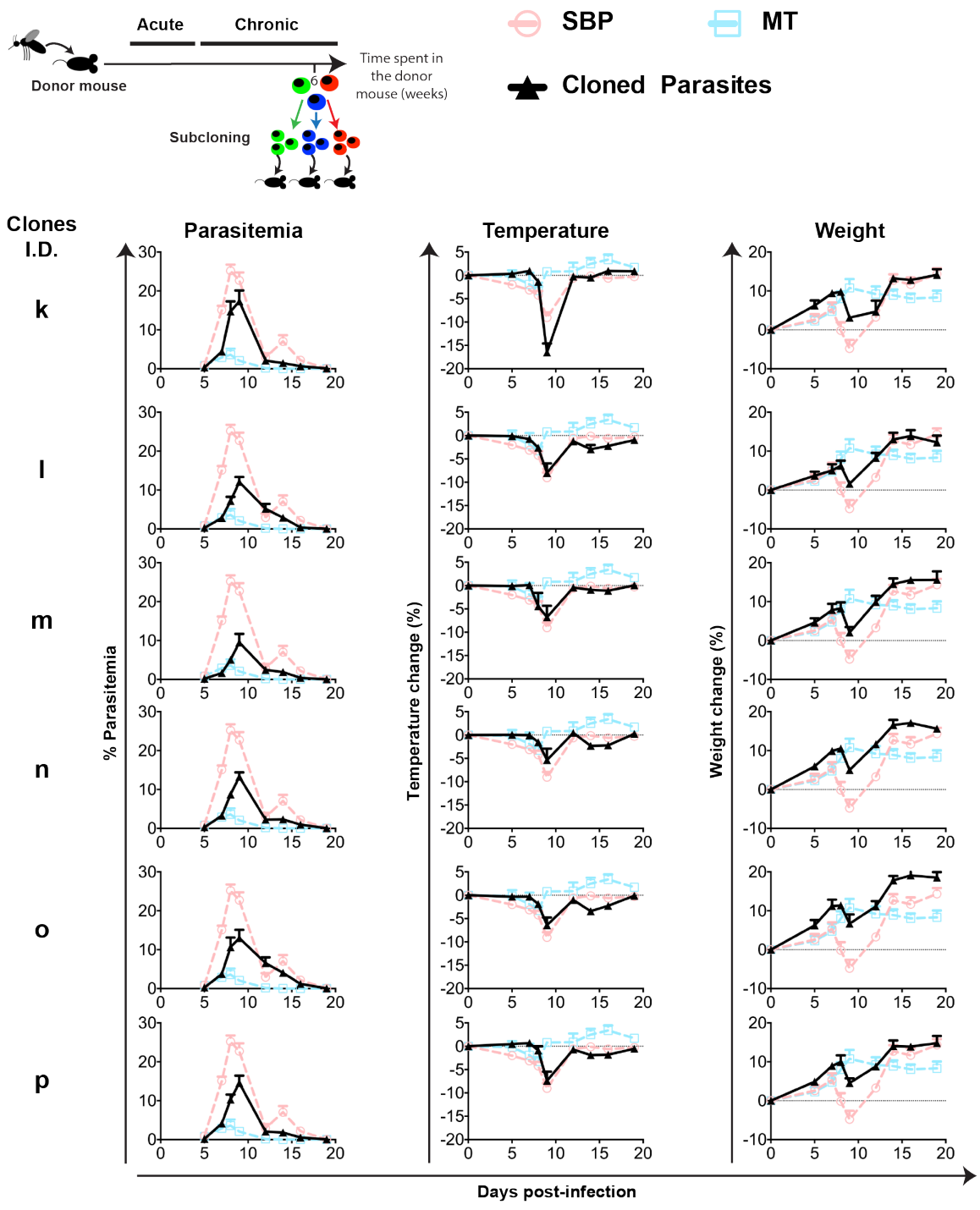

Supplementary Figure 9. Course of infection in mice infected with chronic clones

One donor mouse was infected by mosquito bites. Individual parasites were subsequently cloned during the chronic phase of infection. After their expansion, recipient mice were

130 infected with clonal populations of parasites (n= 5 mice per group). For each clonal
131 infection, we show parasitaemia and changes in temperature and weight over the course
132 of infection in recipient mice compared to mice directly infected by mosquito bites (MT;
133 light blue dotted line) or with serially blood passaged parasites (SBP; light red dotted
134 line). Each dot represents the average ±SEM.

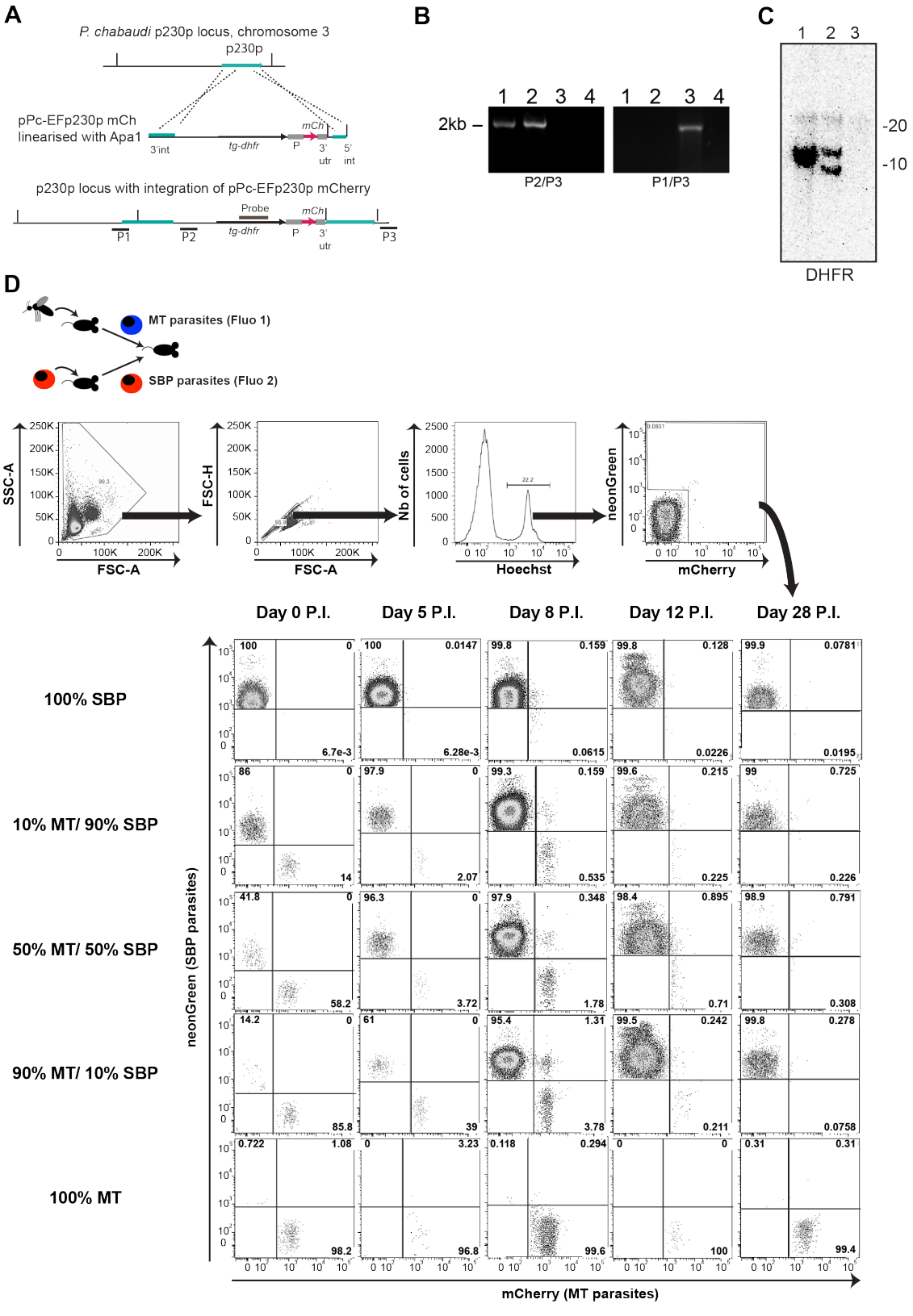
A
P. chabaudi p230p locus, chromosome 3
p230p
pPc-EFp230p mCh
linearised with Apa1
3'int
tg-dhfr
P
mCh
3' utr
5' int
p230p locus with integration of pPc-EFp230p mCherry
Probe
P1
P2
P3
B
1 2 3 4
2kb –
P2/P3
1 2 3 4
P1/P3
C
1 2 3
-20
-10
DHFR
D
MT parasites (Fluo 1)
SBP parasites (Fluo 2)
SSC-A
FSC-A
FSC-H
Nb of cells
Hoechst
neonGreen
mCherry
Day 0 P.I.
Day 5 P.I.
Day 8 P.I.
Day 12 P.I.
Day 28 P.I.
100% SBP
10% MT/ 90% SBP
50% MT/ 50% SBP
90% MT/ 10% SBP
100% MT
neonGreen (SBP parasites)
mCherry (MT parasites)

Supplementary Figure 10. Generation of, and competition between mCherry-tagged MT parasites and NeonGreen-tagged SBP parasites.

(A) The modified p230p locus of chromosome 3 (illustrated for *Pc*EFp230p_mCherry) and the location of PCR primers used to verify integration. (B) PCR verification of integration. Integration of the plasmid was verified with primer set P2/P3 and the loss of the wild type locus shown using primer set P1/P3. Lanes 1-4 contain samples from parasites transfected with *Pc*EFp230p_mCherry (1), *Pc*EFp230p_mNeonGreen (2), *PcAS* wild type parasites (3), water control (4). (C) Southern Blot analysis of EcoRV digested genomic DNA to show integration of *Pc*EFp230p_mNeonGreen and *Pc*EFp230p_mCherry. lane 1, *Pc*EFp230p_mNeonGreen; lane 2, *Pc*EFp230p_mCherry, lane 3 wild-type DNA. TgDHFR probe hybridises to restriction fragments of 12.3 kb and 12.4kb (lane 1) and 9.8 kb and 10.7 kb (lane 2), showing integration (12.3 kb; 9.8 kb) and linearised plasmid (12.4; 10.7) hybrids, respectively. (D) mCherry (Fluo 1) tagged parasites were Mosquito-Transmitted (MT), and neonGreen (Fluo 2) tagged parasites were Serially Blood-Passaged (SBP). Different proportions of the two were used to infect recipient mice by IP injection of 10^5 parasites (n= 10 mice per group). We show the percentages of parasites being SBP or MT as defined by flow cytometry at days 0, 5, 8, 12 and 28 post-infection (P.I.).

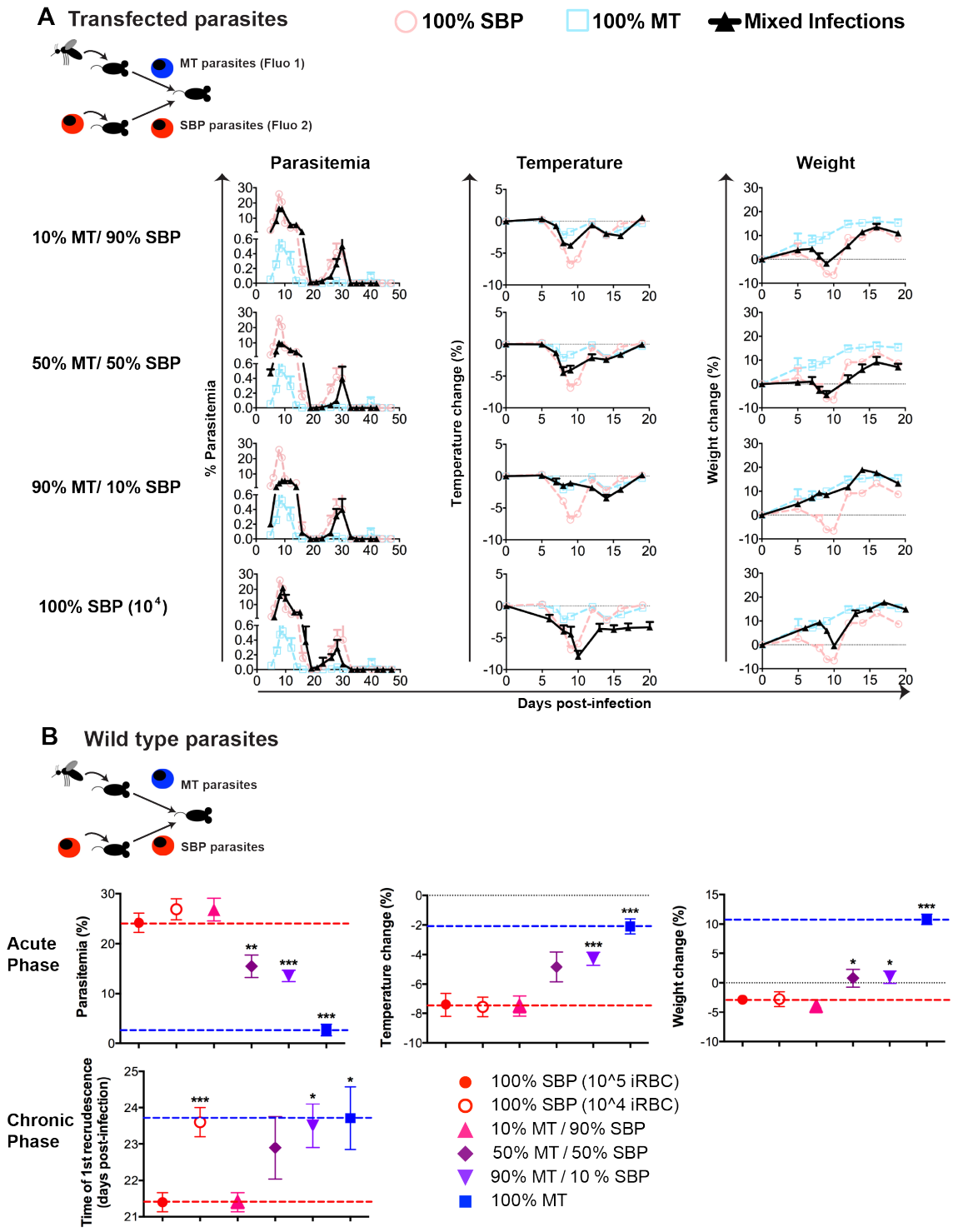

Supplementary Figure 11. Course of mixed infections performed with transgenic and wild type parasites.

(A) mCherry (Fluo 1) tagged parasites were Mosquito-Transmitted (MT), and neonGreen (Fluo 2) tagged parasites were Serially Blood-Passaged (SBP). Different proportions of the two were used to infect recipient mice by IP injection of 10^5 parasites (n= 10 mice per group). As a control, a group of recipient mice was infected by IP injection of 10^4 SBP parasites. We show the parasitaemia and changes in temperature and weight change over the course of infection for each group compared to mice infected with 100% MT parasites (light blue dotted line) or 100% SBP parasites (light red dotted line). Each dot represents the average ±SEM. (B) The same experiment was performed with wild type MT and SBP parasites. We show maximum parasitaemia, temperature change, weight change (upper panel) and time of recrudescence (lower panel) for each group and for mice infected with 100% MT parasites (blue dotted line) or 100% SBP parasites (red dotted line). Each dot represents the average ±SEM. Each group has been compared to mice infected with 10^5 SBP parasites (*P<0,05; **P<0,01; ***P<0,001, two-sided Mann Whitney Test).

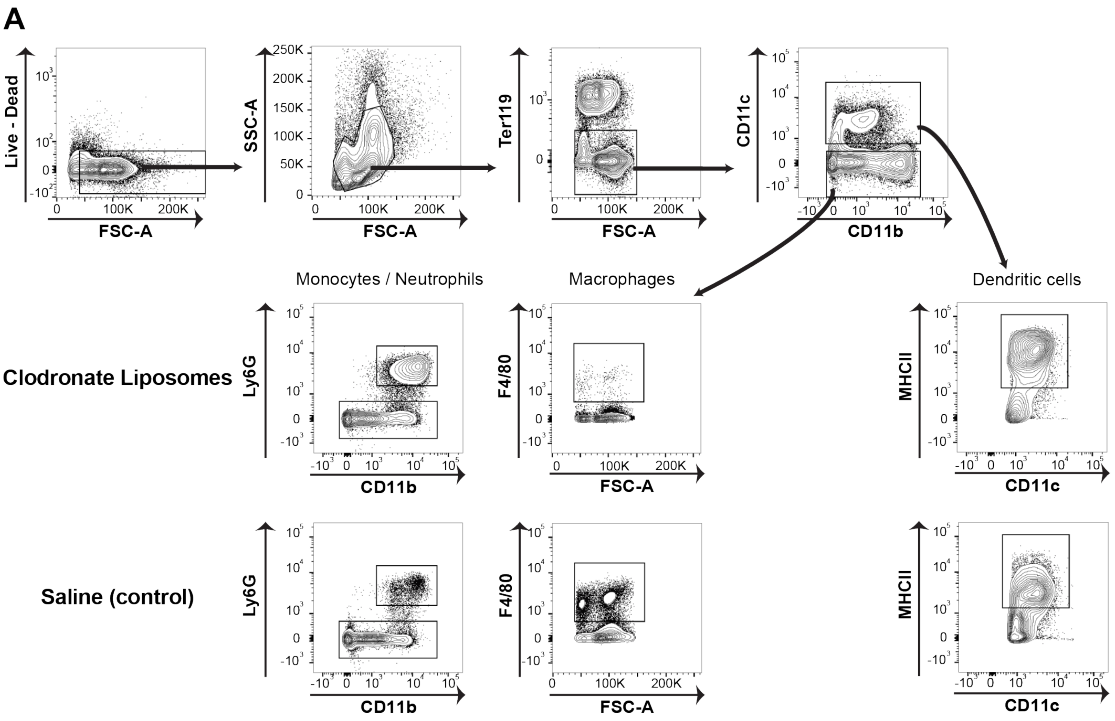

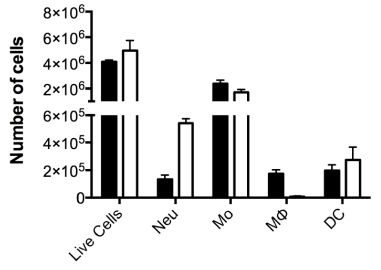

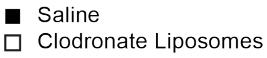

Live	+	+	+	+	+
Lymphocytes	+	+	+	+	+
CD11b	x	+	- /+	- /+	- / +
F4/80	x	-	x	+	-
Ly6G	x	+	-	-	-
CD11c	x	-	-	-	+
MHCII	x	-	x	x	+

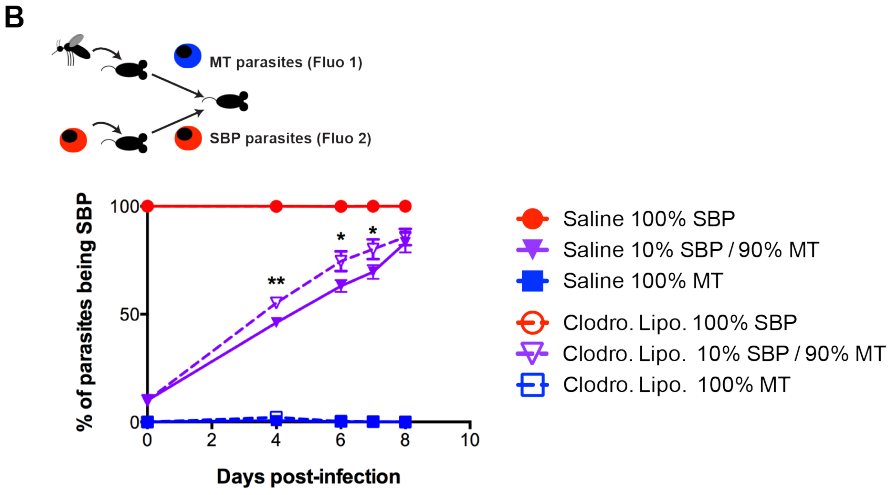

172

Supplementary Figure 12: Competition between SBP and MT parasites in mice deficient of T-, B- and phagocytic cells.

(A) Flow cytometric analysis was performed on splenocytes from B6.RAG-1-/- mice mice 24h after treatment with clodronate liposomes or saline (n=2 per group). The bars represent the total number of each cell type. Gating strategies are shown for Neutrophils (Neu), Monocytes (Mo); Macrophages (MΦ) and Dendritic cells (DC) on the plots and below the chart. (B) mCherry (Fluo 1) tagged parasites were Mosquito-Transmitted (MT), and mNeonGreen (Fluo 2) tagged parasites were Serially Blood-Passaged (SBP). Different proportions of the two were used to infect recipient mice (B6.RAG-1-/- mice treated with saline or clodronate liposomes) by i.p. injection of 10^5 parasites (n= 5 mice per group). The percentage of parasites being SBP (as determined by flow cytometry) is indicated. Each dot represents the average ± standard error of the mean (SEM).

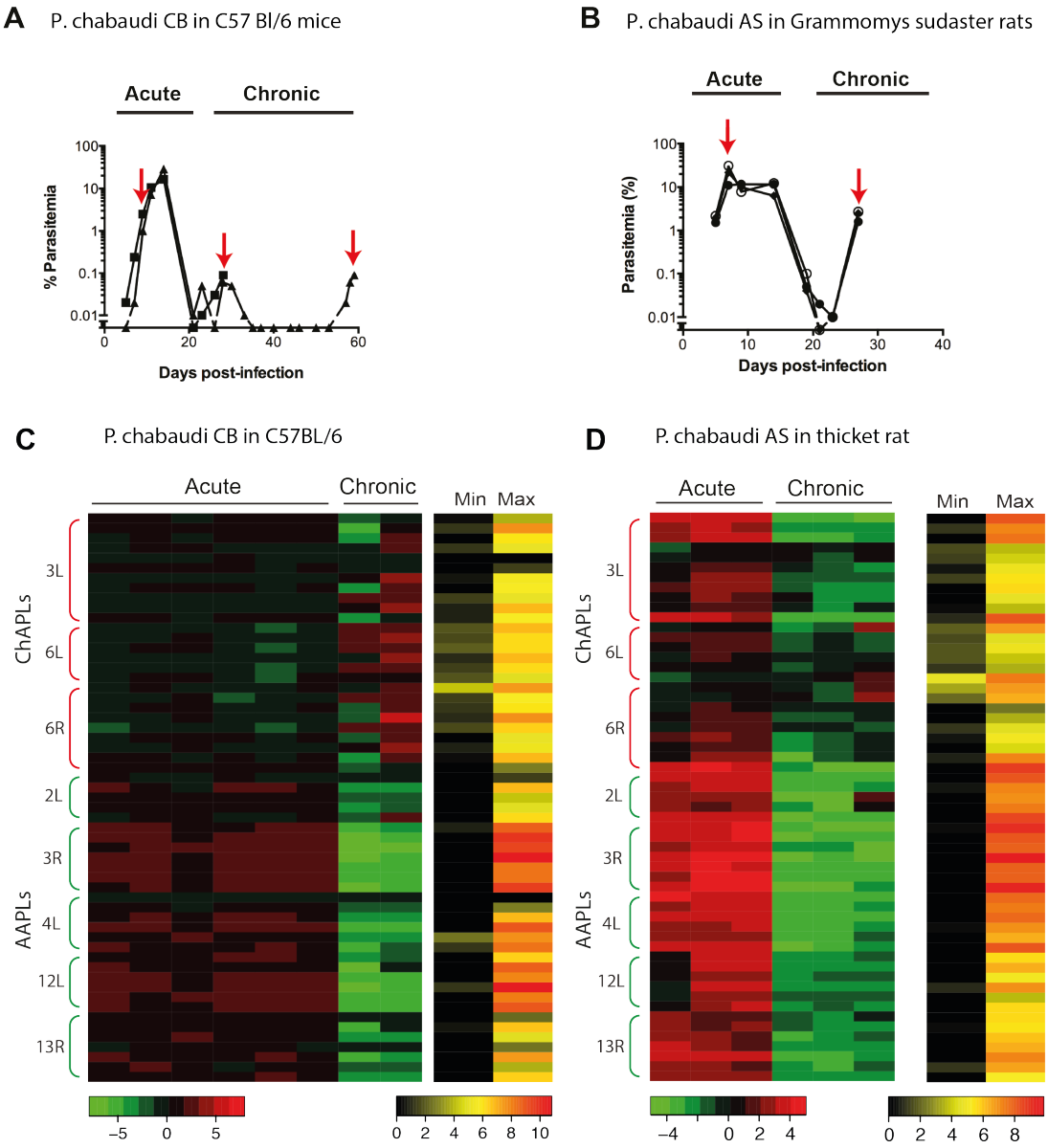

Supplementary Figure 13. Chronic *pir* gene expression in alternative *P. chabaudi* host-parasite systems.

(A) Course of infection of *P. chabaudi* CB in C57Bl/6 mice. Samples were taken where indicated with a red arrow. (B) Course of infection of *P. chabaudi* AS in Grammomys

194 surdater. (C) The CB isolate of *P. chabaudi* has a very similar genome sequence to that of
195 the AS isolate. We observed that the orthologous AAPLs and ChAPLs behave in a very
196 similar way, with 6L and 6R highly expressed during the chronic infection, while AAPL
197 loci were much reduced in expression. (D) Infections of thicket rats with *P. chabaudi* AS
198 again highlighted lower expression of AAPLs and higher expression of ChAPLs during
199 the chronic stage of infection.
200
201

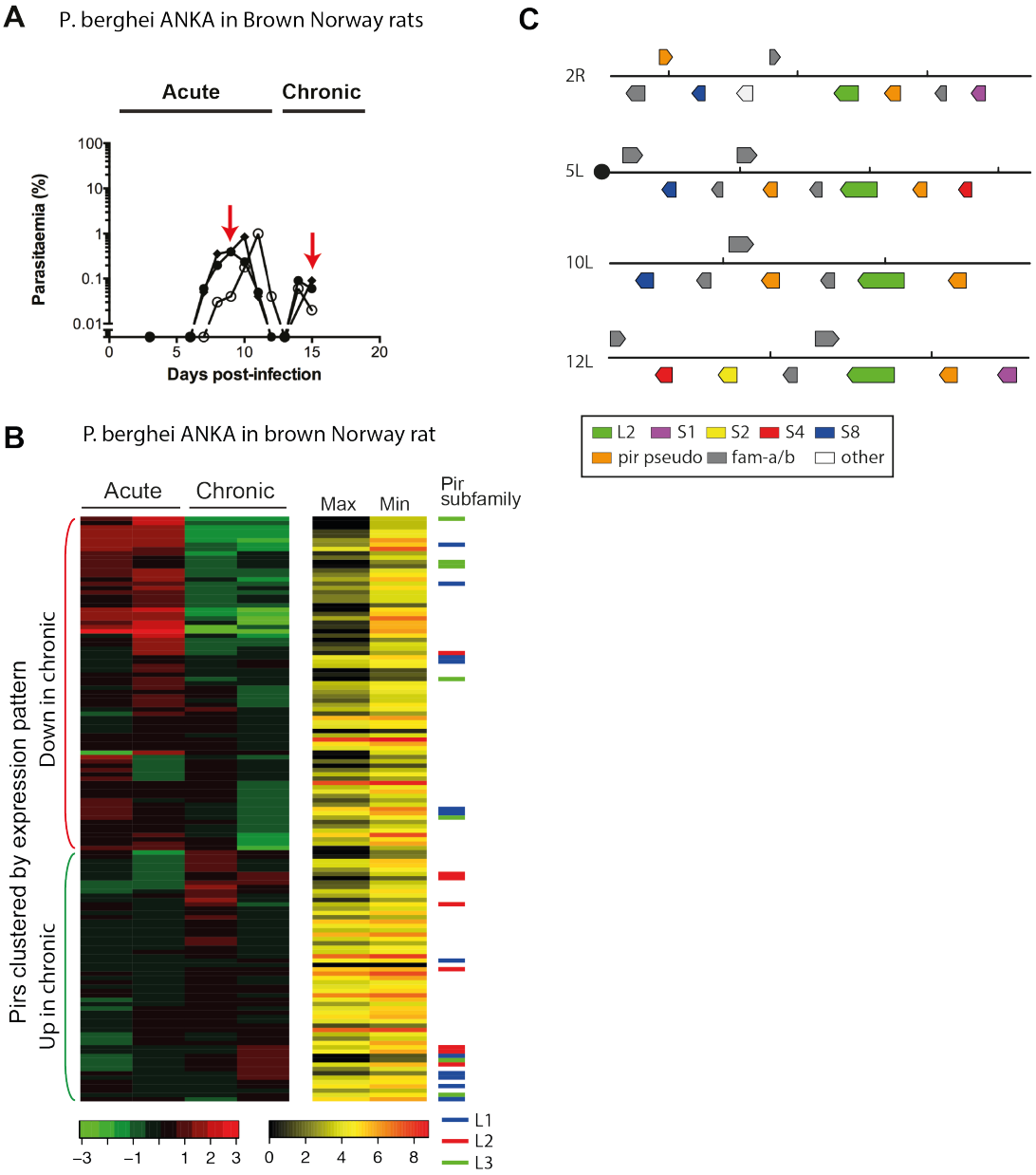

Supplementary Figure 14. Chronic *pir* gene expression in *P. berghei.*

(A) Course of infection of *P. berghei* ANKA in Brown Norway rats. Samples were taken where indicated with a red arrow. (B) *P. berghei* has a significantly diverged repertoire of *pir* genes from *P. chabaudi* and their arrangement in the subtelomeres did not allow identification of gene clusters resembling *P. chabaudi* AAPLs or ChAPLs. However,

during chronic infection of brown rats with this species we observed a general reduced expression of *pir* genes. The small number which we could identify as more highly expressed in chronic infections were enriched for L2 *pirs*, rather than L1s as we saw in *P. chabaudi*. (C) The chronicity-associated L2s we observe in *P. berghei* are from a small number of highly similar loci, which is this respect, are reminiscent of *P. chabaudi* ChAPLs and AAPLs. Furthermore the *P. berghei* L2s have protein sequence features (long variable region, second putative transmembrane domain) more similar to *P. chabaudi* ChAPL L1s than *P. chabaudi* L2s. These results suggest that these L2 genes may perform the same function in *P. berghei* as the ChAPL L1s in *P. chabaudi*.

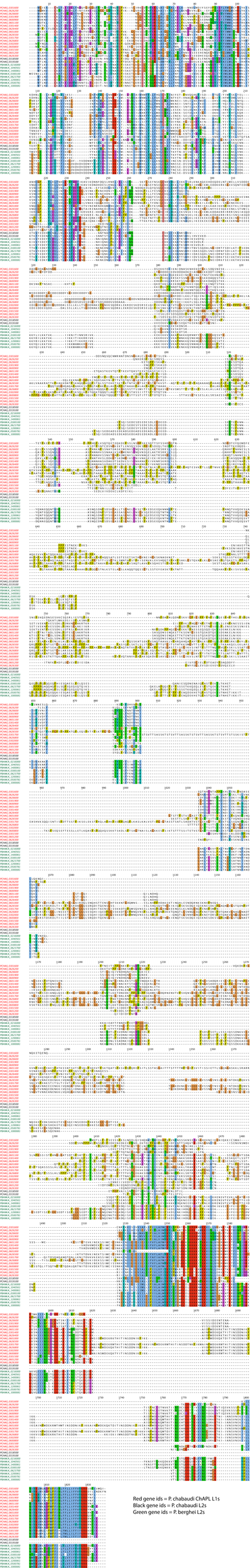

Red gene ids = P. chabaudi ChAPL L1s
Black gene ids = P. chabaudi L2s
Green gene ids = P. berghei L2s

Supplementary Figure 15. Protein sequence alignment of *P. chabaudi* ChAPL L1 *pirs*, L2 *pirs* and *P. berghei* L2 *pirs*.

P. berghei L2 *pirs* share several features with *P. chabaudi* ChAPL L1s. They are the longest *pirs* in the respective genomes. This is due to a long, variable central domain between the highly conserved N and C terminal domains as well as an extended C terminal domain which contains a second putative transmembrane domain.

Supplementary Tables

Supplementary Table 1. Lists of gene differentially expressed between acute and chronic phases for WT, and KO parasites

See Excel file "Supplementary Table 1"

Supplementary Table 2.

Gene family	Genes	DE between acute and chronic in wt mice (%)	Up/Down in chronic	Fold change range
Pir	210	118 (56%)	11/107	-8.5 - +3.6
Fam-a	145	35 (24%)	7/28	-4.6 - +3.8
Lysophospholipase	29	6 (21%)	1/5	-4.3 - +2.7
Fam-c	22	3 (14%)	0/3	-3.6 - +1.4
Fam-b	27	3 (11%)	0/3	-3.7 - -1.1
Fam-d	21	0 (0%)	0/0	n/a

Supplementary Table 3. Comparison of v2 and v3 assemblies of the *Plasmodium chabaudi* AS nuclear genome.

	P. chabaudi AS v2 (*9*)	*P. chabaudi* AS v3 (this work)
Assembly size (Mb)	18.83	18.94
Contigs/chromosomes	37/14	14/14
N50 (Mb)	1.63	1.63
Gaps	3	0
Telomeric sequences/telomeres	14/28	28/28
Pir genes	198	212
Fam-a genes	134	145

Supplementary Table 4. List of genes belonging to AAPL and ChAPL gene clusters. Clusters were defined as those pir genes coexpressed across acute and chronic phases within a particular subtelomere, plus any pir genes not coexpressed, but between coexpressed pirs. These extra genes can be identified by a 'No' in the 'Coexpressed' column.

Locus type	**Locus name**	**Gene id**	***Pir* subfamily**	**Coexpressed?**
ChAPL	3L	PCHAS_0300900	L4	Yes
		PCHAS_0301100	L4	Yes
		PCHAS_0301200	L4	Yes
		PCHAS_0301400	L1	Yes
		PCHAS_0301500	L1	Yes
		PCHAS_0301600	L1	Yes
		PCHAS_0301700	L1	Yes
		PCHAS_0301800	L4	Yes
		PCHAS_0301900	L1	Yes
		PCHAS_0302000	L1	Yes
		PCHAS_0302100	L4	Yes
ChAPL	6L	PCHAS_0600700	L1	Yes
		PCHAS_0600800	L1	Yes
		PCHAS_0600900	L1	Yes
		PCHAS_0601000	L1	Yes
		PCHAS_0601100	L1	Yes
		PCHAS_0601200	L1	Yes
ChAPL	6R	PCHAS_0626200	L1	Yes
		PCHAS_0626300	L1	Yes
		PCHAS_0626400	L1	Yes
		PCHAS_0626500	L1	Yes
		PCHAS_0626600	L1	Yes
		PCHAS_0626700	L4	Yes
		PCHAS_0626800	L1	Yes
		PCHAS_0626900	L4	Yes
		PCHAS_0627100	L4	Yes
AAPL	2L	PCHAS_0200011	L4	Yes
		PCHAS_0200015	S7	Yes
		PCHAS_0200021	S1	Yes
		PCHAS_0200025	S7	Yes
		PCHAS_0200031	L4	Yes
AAPL	3R	PCHAS_0319600	L4	Yes
		PCHAS_0319700	S7	Yes

		PCHAS_0319800	S7	No
		PCHAS_0319900	S7	No
		PCHAS_0320000	S7	Yes
		PCHAS_0320100	L4	Yes
		PCHAS_0320200	S1	Yes
AAPL	4L	PCHAS_0400111	S1	Yes
		PCHAS_0400121	L4	Yes
		PCHAS_0400200	S7	Yes
		PCHAS_0400300	S7	Yes
		PCHAS_0400400	S7	Yes
		PCHAS_0400500	L4	Yes
AAPL	12L	PCHAS_1200200	S7	Yes
		PCHAS_1200300	L4	Yes
		PCHAS_1200400	S7	Yes
		PCHAS_1200500	S7	Yes
		PCHAS_1200600	S7	Yes
		PCHAS_1200700	S7	Yes
AAPL	13R	PCHAS_1370900	L1	Yes
		PCHAS_1371100	L1	Yes
		PCHAS_1371200	S7	Yes
		PCHAS_1371300	S7	Yes
		PCHAS_1371400	S7	Yes
		PCHAS_1371500	S1	No
		PCHAS_1371600	S7	Yes

245

Supplementary Table 5. Expression levels of *pir* genes during chronic and acute stages of infections of wild type mice, B6μMT, B6.TCRα-/- mice with *P. chabaudi* AS, wild type mice with *P. chabaudi* CB, brown rat with *P. berghei* and *Grammoymys surdaster* with *P. chabaudi* AS.

See Excel file "Supplementary Table 5.xlsx".

Supplementary Table 6. Expression levels of *pir* genes in cloned parasite lines

See Excel file "Supplementary Table 6.xlsx".

Supplementary Table 7. Genes where expression level during the acute phase was correlated with the time at recrudescence.

See Excel file "Supplementary Table 7.xlsx".

Supplementary Table 8. Primer sequences used to verify integration of plasmid constructs.

Primer	Sequence
P1	TATCTATAAGGGAAGATACTCAT
P2	GTAAAGGGTTAATTCTTATATG
P3	CTTCTATGTTGGATACACTTTGC

Supplementary Table 9. Differentially expressed *pir* genes in *P. berghei* chronic infections. We compared both acute and both chronic samples with an FDR < 0.1 and then both acute samples against each of the chronic samples individually with the same cutoff. This allowed for that fact that we have relatively few replicates and therefore low statistical power as well as that we expect *pir* changes not to be consistent between replicates as this is what we observed in *P. chabaudi*. We find that while L2s are always upregulated in chronic infection, they are never downregulated.

	Pir subfamily	**Acute vs. Chronic**	**Acute vs. Chronic 1**	**Acute vs. Chronic 2**
Pirs up in chronic	Pseudogenes	1	2	1
	L1			1
	L2	1	1	4
	L3			
	S1		2	
	S2			
	S4			
	S5			
	S8		1	
Pirs down in chronic	Pseudogenes	2	2	8
	L1	4	6	4
	L2			
	L3	1	1	1
	S1	5	5	10
	S2	4	4	6
	S4	2	2	6
	S5			
	S8		1	2

Supplementary Table 10. RNA-seq libraries used in the study.

All samples are from blood stage parasites isolated at 11:00 (reverse light cycle), when >90% of the parasites were at the late trophozoite stage of development. In the sample names T1 = acute phase and T2 = chronic phase, while numbers such as 21-1 refer to a particular mouse, so T1_21-1 and T2_21-1 refer to acute and chronic phase samples from mouse 21-1. The library type column describes the fragment size of the library e.g. 200-450bp, the number of PCR cycles e.g. 10 and the type of sequencing e.g. 100bp PE = 100bp read lengths from both ends of the fragment. Description includes point of infection (acute = peak parasitaemia, chronic = first recrudescence), host genotype (*Mus musculus* C57BL/6 B6.wt = wild type, B6.μMT-/-, B6.TCRa-/-; Gs = *Grammomys surdaster*; Rn = *Rattus norvegicus*), and parasite isolate/species (AS = P. c. chabaudi AS; CB = *P. chabaudi* CB; Pb = *P. berghei* ANKA) and clone name for the cloned samples**.**

Sample name	**Accession number**	**Library type**	**Description**	**Days post infection**	**% parasitaemia**	**% rings**	**% trophozoites**	**% schizonts**	**% gametocytes**
T1_20-14	ERS346505	200-450, 10, 100bp PE	Acute, B6.wt, AS	9	3.13	1	98	1	0
T1_21-1	ERS346506	200-450, 10, 100bp PE	Acute, B6.wt, AS	9	1.3	0	99	1	0
T1_21-2	ERS346508	200-450, 10, 100bp PE	Acute, B6.wt, AS	9	1.16	1	97	2	0
T1_21-4	ERS346513	200-450, 10, 100bp PE	Acute, B6.wt, AS	9	3.59	1.6	97.6	0.8	0
T1_21-14	ERS346519	200-450,	Acute,	9	1.95	8	89	3	0

		10, 100bp PE	B6.wt, AS						
T2_20-14	ERS346512	200-450, 10, 100bp PE	Chronic, B6.wt, AS	34	0.17	1	99	0	0
T2_21-1	ERS346510	200-450, 10, 100bp PE	Chronic, B6.wt, AS	43	0.2	4	96	0	0
T2_21-2	ERS346509	200-450, 10, 100bp PE	Chronic, B6.wt, AS	39	0.22	0	99	0	1
T2_21-4	ERS346504	200-450, 10, 100bp PE	Chronic, B6.wt, AS	32	0.62	1	98	0	1
T2_21-14	ERS346499	200-450, 10, 100bp PE	Chronic, B6.wt, AS	36	0.33	0	98	0	2
T1_42-1	ERS423636	200-450, 10, 100bp PE	Acute, B6.wt, AS	9	8.8	1	99	0	0
T1_42-7	ERS423642	200-450, 10, 100bp PE	Acute, B6.wt, AS	9	9	4.5	95.5	0	0
T1_43-2	ERS423654	200-450, 10, 100bp PE	Acute, B6.μMT, AS	9	7.2	1.5	98.5	0	0
T1_43-6	ERS423656	200-450, 10, 100bp PE	Acute, B6.μMT,	9	10.5	1	99	0	0
T1_45-2	ERS423647	200-450,	Acute,	9	2.64	0.5	99.5	0	0

		10, 100bp PE	B6.wt, AS						
T1_45-6	ERS423649	200-450, 10, 100bp PE	Acute, B6.wt, AS	9	3.6	1.5	98.5	0	0
T1_46-4	ERS423657	200-450, 10, 100bp PE	Acute, B6.μMT, AS	9	6.05	25	74.5	0.5	0
T1_46-6	ERS423638	200-450, 10, 100bp PE	Acute, B6.μMT, AS	9	11.2	7.5	92.5	0	0
T1_47-1	ERS423644	200-450, 10, 100bp PE	Acute, B6.TCRα-/-, AS	9	8.25	3	97	0	0
T1_47-2	ERS423650	200-450, 10, 100bp PE	Acute, B6.TCRα-/-, AS	9	4.18	5	94.5	0.5	0
T1_47-4	ERS423655	200-450, 10, 100bp PE	Acute, B6.TCRα-/-, AS	9	33.7	4.5	95.5	0	0
T2_42-1	ERS423640	200-450, 10, 100bp PE	Chronic, B6.wt, AS	31	0.42	0	100	0	0
T2_42-7	ERS423637	200-450, 10, 100bp PE	Chronic, B6.wt, AS	30	0.2	0	98	0	2
T2_43-2	ERS423645	200-450, 10, 100bp PE	Chronic, B6.μMT, AS	52	3.2	0	100	0	0
T2_43-3	ERS423639	200-450,	Chronic,	64	1.68	0.5	99	0.5	0

		10, 100bp PE	B6.μMT, AS						
T2_43-6	ERS423648	200-450, 10, 100bp PE	Chronic, B6.μMT, AS	73	2.05	3	96.5	0	0.5
T2_45-2	ERS423641	200-450, 10, 100bp PE	Chronic, B6.wt, AS	33	0.12	0	100	0	0
T2_45-4	ERS423653	200-450, 10, 100bp PE	Chronic, B6.wt, AS	30	0.26	4	96	0	0
T2_45-6	ERS423658	200-450, 10, 100bp PE	Chronic, B6.wt, AS	34	0.21	2	98	0	0
T2_46-4	ERS423652	200-450, 14, 100bp PE	Chronic, B6.μMT, AS	59	1.1	2	97	0	1
T2_46-6	ERS423646	200-450, 10, 100bp PE	Chronic, B6.μMT, AS	33	0.26	4	96	0	0
T2_47-1	ERS423659	200-450, 10, 100bp PE	Chronic, B6.TCRα-/-, AS	30	6.26	4.5	95.5	0	0
T2_47-2	ERS423651	200-450, 10, 100bp PE	Chronic, B6.TCRα-/-, AS	30	12.54	0	100	0	0
T2_47-4	ERS423643	200-450, 14, 100bp PE	Chronic, B6.TCRα-/-, AS	30	29	2	96	1.5	0.5
53-1	ERS792706	100-300,	Acute,	7	1.04	3	97	0	0

		10, 75bp PE	B6.wt, AS, clone f						
53-2	ERS792707	100-300, 10, 75bp PE	Acute, B6.wt, AS, clone f	7	2.7	3	96	1	0
53-3	ERS792708	100-300, 10, 75bp PE	Acute, B6.wt, AS, clone f	7	3.55	1	99	0	0
54-1	ERS792709	100-300, 10, 75bp PE	Acute, B6.wt, AS, clone a	7	0.86	0	90	7	3
54-2	ERS792710	100-300, 10, 75bp PE	Acute, B6.wt, AS, clone a	7	2.3	3	91	6	0
54-3	ERS792711	100-300, 10, 75bp PE	Acute, B6.wt, AS, clone a	7	1.8	0	100	0	0
55-1	ERS792712	100-300, 10, 75bp PE	Acute, B6.wt, AS, clone b	7	2.4	0	99	1	0
55-2	ERS792713	100-300, 10, 75bp PE	Acute, B6.wt, AS, clone b	7	7.9	5	91	2	2
55-3	ERS792714	100-300, 10, 75bp PE	Acute, B6.wt, AS, clone b	7	0.07	0	100	0	0
56-1	ERS792715	100-300, 10, 75bp PE	Chronic, B6.wt, AS, clone k	7	2	1	97	1	1
56-2	ERS792716	100-300,	Chronic,	7	2.2	21	73	5	1

		10, 75bp PE	B6.wt, AS, clone k						
56-3	ERS792717	100-300, 10, 75bp PE	Chronic, B6.wt, AS, clone k	7	3.3	29	61	10	0
57-1	ERS792718	100-300, 10, 75bp PE	Chronic, B6.wt, AS, clone n	7	0.67	4	90	4	2
57-2	ERS792719	100-300, 10, 75bp PE	Chronic, B6.wt, AS, clone n	7	2.65	33	64	3	0
57-3	ERS792720	100-300, 10, 75bp PE	Chronic, B6.wt, AS, clone n	7	3.4	5	90	3	2
58-1	ERS792721	100-300, 10, 75bp PE	Chronic, B6.wt, AS, clone p	7	2.8	11	88	1	0
58-2	ERS792722	100-300, 10, 75bp PE	Chronic, B6.wt, AS, clone p	7	14.7	1	98	0	1
58-3	ERS792723	100-300, 10, 75bp PE	Chronic, B6.wt, AS, clone p	7	6.2	3	94	2	1
MTCB1	ERS1390889	100-300, 15, 75bp PE	Acute, B6.wt, CB	7	7.9	17.3	77.8	4.6	0.2
MTCB2	ERS1391216	100-300, 15, 75bp PE	Acute, B6.wt, CB	7	19.3	14.9	83.3	1.4	0.4
MTCB3	ERS1391219	100-300,	Acute,	7	7.4	17.6	81.6	0.6	0.2

		15, 75bp PE	B6.wt, CB						
MTCB4	ERS1391221	100-300, 15, 75bp PE	Acute, B6.wt, CB	7	10.1	8.2	91.3	0.4	0
MTCB5	ERS1391557	100-300, 15, 75bp PE	Acute, B6.wt, CB	7	9.2	8.9	91.1	0	0
MTCB6	ERS1391598	100-300, 15, 75bp PE	Acute, B6.wt, CB	7	11.2	11	88.0	0.88	0
T2_05_6	ERS1348217	100-300, 10, 75bp PE	Chronic, B6.wt, CB	59	0.09	0	100	0	0
T2_05_10	ERS1348218	100-300, 10, 75bp PE	Chronic, B6.wt, CB	28	0.09	3	97	0	0
681_T1	ERS1348224	100-300, 10, 75bp PE	Acute, Gs, AS	9	11	0	100	0	0
701_T1	ERS1348225	100-300, 10, 75bp PE	Acute, Gs, AS	9	21.67	0	100	0	0
703_T1	ERS1348226	100-300, 10, 75bp PE	Acute, Gs, AS	9	31	0	100	0	0
681_T2	ERS1348227	100-300, 10, 75bp PE	Chronic, Gs, AS	27	1.6	0	100	0	0
701_T2	ERS1348228	100-300,	Chronic, Gs,	27	2.5	0	100	0	0

		10, 75bp PE	AS						
703_T2	ERS1348229	100-300, 10, 75bp PE	Chronic, Gs, AS	27	2.5	0	100	0	0
PbBN1_T1	ERS1348206	100-300, 10, 75bp PE	Acute, Rn, Pb	10	0.69	20	80	0	0
PbBN2_T1	ERS1348207	100-300, 10, 75bp PE	Acute, Rn, Pb	10	1.36	20	79	0	1
PbBN1_T2	ERS1348208	100-300, 10, 75bp PE	Chronic, Rn, Pb	15	0.06	30	70	0	0
PbBN2_T2	ERS1348209	100-300, 10, 75bp PE	Chronic, Rn, Pb	15	0.0.9	30	70	0	0